NASA Technical Memorandum 106138

Calibration of a Shock Wave Position Sensor Using Artificial Neural Networks

Arthur J. Decker and Kenneth E. Weiland
Lewis Research Center
Cleveland, Ohio

May 1993

NASA

CALIBRATION OF A SHOCK WAVE POSITION SENSOR USING ARTIFICIAL NEURAL NETWORKS

Arthur J. Decker and Kenneth E. Weiland
National Aeronautics and Space Administration
Lewis Research Center
Cleveland, Ohio 44135

SUMMARY

This report discusses the calibration of a shock wave position sensor. The position sensor works by using artificial neural networks to map cropped CCD frames of the shadows of the shock wave into the value of the shock wave position. This project was done as a tutorial demonstration of method and feasibility. It used a laboratory shadowgraph, nozzle, and commercial neural network package. The results were quite good, indicating that artificial neural networks can be used efficiently to automate the semiquantitative applications of flow visualization.

INTRODUCTION

Aeronautics has always had a need to record and to use flow visualization and other whole field or "picture" data. Prelaser sources of flow visualization included schlieren, shadowgraphy, and interferometry. The invention of the laser added holography, fluorescence spectroscopy, and lately particle image velocimetry. Utilization improved greatly in the 1980's with the development and marketing of inexpensive, powerful PCs and workstations at the low end of computing and supercomputers at the high end. Rapid, parallel measurements of optical interference phase from interferograms are now common. Velocimetry from double images of moving particles is another example of a whole field method. Beautiful visualizations from computed and measured data grace the pages of magazines. Yet these developments are not very easy to use for aeronautical tests and experiments, and there is a straightforward reason for this defect.

Most automated recording, processing, and utilization of optical data, and optical image data in particular, require heavy intellectualization from start to finish. Electronic interferometry, for example, rapidly produces a map of the interference phase from a test object. Nevertheless, every effect on the interference phase from source to sensor must be considered. Changes in optical alignment and in the optical path have significant effects which are difficult to monitor. The data, once recorded, requires possibly complex and lengthy manipulations. These requirements are tolerable in a laboratory or carefully designed experiment where conditions can be controlled and time is not of the essence, but are very difficult in the field.

The automated recording and processing of the semiquantitative or "picture" data of classical flow visualization is certainly no easier. The applications of image processing require the use of a collection of heuristics, ad hoc algorithms, and the like. A task such as tracing out the shape of a flow feature or unwrapping and plotting the phase contours from an interferogram is difficult.

The growing technology of artificial neural networks offers a possibly more practical alternative, particularly for the use of optical data in operations but also for some kinds of data processing. Artificial neural networks allow a user of optical technology to create a custom made calibration between picture data and a flow property or control action, for example. The calibration is done by example in a process called training. A good choice of training examples may depend on the experience and judgement of the

user or operations person, but does not require much knowledge of optics or the detailed effects on the light rays detected by the sensor array. The process that maps a picture into a property or control action is implicit. Detailed knowledge of that process is not necessary and may not even be possible or desirable.

NASA Lewis Research Center has sufficient faith in the future applications of artificial neural networks and related technologies to be testing them on at least four applications: automated alignment of optical measurement instrumentation (refs. 1 to 5); processing of optical data (ref. 6); automation of certain operations of a supersonic wind tunnel; and control (ref. 7). This faith is based not on any new knowledge, since the concepts behind artificial neural networks have been under development since the early 1940's (ref. 8). The allied field of fuzzy sets was introduced in 1965 (ref. 9). Rather we expect a growing selection of commercially available software, hardware, and affordable computer technology dedicated to neural networks (ref. 4) will make their application more practical and affordable in real situations.

This paper discusses the results of a mini-project, which was done in the spirit of a tutorial, on picture-to-property calibration using neural networks. An input picture for this demonstration is a CCD recording of the shadow of a shockwave from a supercritically operated converging nozzle. The output property is the shockwave position as defined later. This choice of subject is particularly appropriate considering the interest in rapid sensing of shock wave positions (ref. 10). Training and test sets of distinct input-picture, output-position combinations were generated by varying the nozzle pressure. There was no effort to control the quality of the flow visualization or the properties of the nozzle. The results are surprisingly good and, we hope, demonstrate the potential utility of using neural net calibrations for as-is situations in the field.

The paper begins with a brief discussion of the equipment. That discussion is followed by the calibration procedure, results, and conclusions.

APPARATUS

The equipment for this demonstration included: a supercritically operated converging nozzle (ref. 11); a shadowgraph (ref. 12); a CCD camera (ref. 13); a PC mounted frame grabber board (ref. 14); and a graphics workstation (ref. 15) with commercial neural network software (ref. 16). Much of this equipment is part of a permanent setup used for another application, and was convenient for this demonstration. A real sensor probably would not use a workstation; it might incorporate neural net hardware rather than software.

The nozzle was a 0.25-in. (6.4-mm) o.d. copper tube crimped to a slot orifice which turned out to be 1.0 by 6.2 mm. A CCD frame of a shadow of the tube and accompanying shock pattern is shown in figure 1. The pressure in the tube was varied between 65 and 120 psig in order to move the shock pattern relative to the nozzle. The location of the shock wave nearest the nozzle varied significantly as the pressure was changed. The nozzle was not made particularly carefully; it's only purpose was to effect this demonstration.

A shadowgraph was used for flow visualization. There is a relationship in shadowgraphy between the shadow pattern of a shock wave and the location of the shock front. Shock waves are associated with the rather broad patterns of dark and bright bands in figure 1. The shock front is identified with the edge of a dark shadow. Hence, the edge of the dark shadow nearest the nozzle was defined as the location of the shock front for this demonstration, and only that portion of the shock pattern was used to train the neural network.

Figure 2 is a schematic of the shadowgraph including the CCD camera that was used to record the images. Again no special care was used in constructing the shadowgraph or positioning the camera, and diffraction and other artifacts are clearly present in Fig. 1. We simply adjusted the image of the tube's shadow to occupy about 20 percent of the width of the frame. We have also used focusing schlieren and double-exposure holography for this general kind of exercise. The results for these flow visualization methods have been acceptable for a wide variety of image qualities.

The images were acquired by a frame grabber in a PC. The frame grabber stores a 512- by 480-element image. The frame grabber and software have image processing capability, and neural network packages can be written or purchased for the PC. Nevertheless, we chose for convenience to send the binary images to a graphics workstation to complete the demonstration. The workstation has a variety of image processing and computational software as well as an easy-to-use, commercial, neural net package.

Artificial neural networks (networks of parallel and interconnected processing elements) have long been extant, but only recently common. One can choose to learn much detail from books and the literature (refs. 17 to 19), or little detail by referring only to the manuals supplied with a commercial package, without affecting an application very much. Figure 3 shows a feed-forward network of the general kind used for this demonstration. The circles denote nodes and the lines weighted connections. "Feed forward" means that a vector of data applied at the input nodes is transmitted forward from left to right through subsequent connections and nodes to the outputs. Effectively, a vector of input information is mapped onto a vector of output information. The input and output vectors can have different sizes.

The key application of the feed-forward network is to learn the function that maps a set of inputs (the domain) onto a set of outputs (the range). This function is learned implicitly: a trained network will perform the function, but will not provide an explicit expression for it. A network can learn a general function if it has at least one hidden layer of nodes (a layer besides the input and output layers). The application is only slightly more complicated if the input-output relationship is stochastic as with real measurements. Then the network can be trained to perform about as well as a Bayes limited classifier (ref. 20).

The first step in training a neural network is to select a representative training set which is nothing more than a table of output vectors versus input vectors. Our input vectors are cropped CCD pictures of the shock wave and surrounding region. Our output vectors contain a measurement of the position of the shock wave made as described later.

The second step is to select a test set of input-output vectors. This step is essential, since there is no absolute criterion for deciding when a neural network has trained adequately. Typically, the difference between training outputs and actual outputs is monitored during training. Various ways of monitoring this difference are provided by writers of neural network training packages. The operator chooses to terminate training when the difference is small enough or is not continuing to decrease in the operator's judgement. The test set is then applied, and the operator judges whether the outputs are adequate.

The third step is to select the neural network architecture. The menu driven, commercial package used for this demonstration contained a variety of architectures and training algorithms. We selected a modified feed-forward network. This kind of selection is typical and generally satisfactory, in spite of the variety of choices available. Two input formats were tested. One format used a 52- by 55-element cropped CCD picture that had been converted from binary to analog. Hence, 2860 input nodes were required. Figure 4 shows the training inputs, where each frame differs from the previous frame by a 2-psi pressure increment. The pressures are in the range from 70 to 114 psig. The frames were subjected to some contrast enhancement for the benefit of the reader and the person measuring the location of the shock front. Said enhancement is not essential for the neural network. The second format was a 5- by 52-element frame chosen to

simulate a line detector, and figure 6 shows the training inputs. The line images were selected at the same pressures as for the 52- by 55-element case. The frame bottoms are cropped just at the nozzle level.

Two formats were selected for the output vector which contains a measurement of the position of the shock wave. One output format was a six-bit binary number requiring six nodes. The second format was an analog number requiring one node. The position was measured where a line parallel to the vertical axis intersected the shock front. The line was chosen near the left edge, but where the curvature of the shock front does not change significantly with pressure. The position was defined to be the distance in pixels above the nozzle.

The hidden layer was chosen to contain six nodes. There is no magic formula for the selection of the number of hidden layers or the selection of the number of nodes in a hidden layer. Presently readily available technology is well suited to connecting a large number of inputs to relatively few hidden nodes and output nodes. The standard architecture fans out the output of each node into a separate weighted input at each node in the subsequent layer. A node then sums its weighted inputs and a bias term; uses the sum as the argument of a nonlinear function; and uses the value of the function as the output to be fanned out to nodes in the next layer. The output of an output node is, of course, an element of the output vector. Our architecture differed from the standard in that the output layer also received inputs from the input layer as well as the hidden layer.

The construction of the neural network sounds complicated, but is accomplished quickly by an operator using the menus supplied with the software package used. The training procedure is a little more difficult, but can also be accomplished by the operator. Training is effectively the same as instrument calibration. This calibration procedure is discussed in the next section.

CALIBRATION AND TRAINING

Calibration requires that an instrument output be adjusted to replicate accurately the input-output pairs of standards. One also assumes that the instrument will perform accurately at nonstandard points within the domain and range of calibration. One is also gratified if the instrument can be extrapolated somewhat outside the domain and range of calibration. We seek nothing more than this for the neural net shock wave sensor and similar instruments.

Our objectives are to show: (1) that the neural network can learn the training examples precisely; (2) that the neural network can process inputs accurately in the range and domain of the training examples; and (3) that the neural network can extrapolate somewhat outside the domain and range of training.

One training set consisted of the 23 pictures of shock waves shown in figure 4 and the corresponding shock wave position measurements. The position or distance above the nozzle was measured at only one point on the shock front for each picture. A more detailed study would have measured the shock position at several points on the shock front or provided the coefficients of a curve fit of the shock front. The pressure in figure 4 increases from the upper left to the lower right.

The measurement point was defined only approximately for the frames of figure 4. There is a relatively flat portion of the shock front near the left edge of each frame. The measurement of the distance of this region above the nozzle was accomplished by cropping the frame a horizontal line at a time until the crop line was exactly at the bottom of the dark shadow of the shock wave in this region. The distance of the

crop line above the bottom of the frame was then read in lines. The separation between lines is about 50 μm. The workstation has software that can easily be used to perform this kind of measurement. The estimated random error was no worse than plus or minus one line.

Each training picture was converted from binary pixels to ASCII encoded pixels and concatenated with a position measurement to form a training record. The distance of the shock position above the nozzle varied from 19 to 46 lines as the pressure was varied from 65 to 120 psig. Training was actually accomplished in the range from 70 to 114 psig. We stated in the previous section that two formats were tested for the output vector. In one case, a binary number of six bits, translating into six output nodes, was used. A distance of 33 lines would then be represented as 1, 0, 0, 0, 0, 1. The second format consisted of an analog number. The 23 training records were then concatenated into a training set in a manner prescribed by the commercial neural network package.

The second objective, performing interpolation, was tested with a test set. The test set, shown in figure 5, looks much like the training set. It corresponds to pressure settings in between the training points, and was measured and formatted in exactly the same way as the training set. The test set contains 23 records.

Test records were also prepared at 65 and 120 psig to test the third objective: extrapolation.

Training and test sets of 5- by 55-element inputs were also prepared as stated in the previous section (figs. 6 and 7). The objective was to simulate a line detector. The location of the line detector was the same for each frame and was located in the measurement region defined above. The shock position was remeasured from each line image. The operator claimed that this measurement was harder than with the 52- by 55-element picture. There was a systematic difference between the position measurements for the 52- by 55-element and 5- by 55-element frames, particularly at the higher pressures.

Neural networks were trained with the two input formats and the two output formats for a total of four training sessions. Selecting a training algorithm, training schedule, and training criteria is quite different from choosing the network architecture and training set. The result of training in the limit should be the same regardless of the training algorithm as stated in connection with the Bayes theorem in the previous section. Training typically is slow. Much research and development in neural networks involves finding faster training algorithms. We selected a modified backpropagation algorithm from the menus supplied with our package. There is no point in discussing the often ad hoc theories of training: they are discussed in the references, and their details, although interesting, complicate our demonstration too much. We state only that training involves iterative changes of the network weights until the differences between the training outputs and the actual outputs of the network are small enough. The software package performs these actions automatically once the training parameters have been chosen. Some trial and error may be required to choose the right parameters, and training may take a long time: we used some overnight training sessions for this demonstration. Fortunately, PCs and workstations do not complain about working conditions.

The selection of a training error criterion is a little easier to discuss. The outputs of the networks are integers: 0's and 1's in the binary case and integers between 19 and 48 (lines) in the analog case. One output node is used for each binary digit, and only one output node is used for the analog case. In fact, the network requires normalized data either from -1.0 to 1.0 or 0.0 to 1.0, since the nonlinear activation function mentioned in the previous section operates between these limits. An activation function between 0.0 and 1.0 is used for the positive outputs of this demonstration. The decimal point is included not for significance, but to indicate that the output will be a decimal number. There may be many significant figures. Actually, the data is normalized in the range from 0.2 to 0.8. The reason is that the nonlinear

functions do not reach 0.0 and 1.0 until their arguments are at minus or plus infinity. The smaller range keeps the weights within attainable values. Normalization and denormalization were performed automatically by the software package. The outputs of the network are rounded up or rounded down to integers: 0's and 1's in the binary case and twin digit integers in the analog case. The software package provides a running rms error averaged for the number of nodes and training records. That error should be significantly smaller than 0.4 to reduce the probability of erroneous rounding of a binary digit. We selected a value of 0.1 or less. The criterion is more stringent for the analog output. There, the error of the normalized output (there was only one node) should be less than 0.01. Again, the error is calculated from the differences between the normalized training outputs and the actual normalized outputs of the network.

The results of calibration are shown and discussed in the next section.

RESULTS AND DISCUSSION

The results of training and testing are shown in figures 8 to 12. Figures 8 to 11 represent training sessions which meet the training error criteria discussed in the previous section. For comparison, figure 12 shows results for a network which was trained for a short time and was not allowed to meet the training error criterion.

The figures all have the same format. The solid curve shows the manually measured shock front positions. The positions are expressed in pixels above the nozzle, where a pixel dimension or vertical line spacing is about 50 μm. The horizontal axis actually shows frame labels. Recall that frames were recorded in 1-psi increments beginning at a nozzle pressure of 70 psig. The solid points are positions generated by the neural network in response to the frame inputs. There are 46 points shown covering the pressure range from 70 to 115 psig. The small points are training points, and the large points in between are test points. There are 23 training points and 23 test points.

Figures 8 and 9 show results for the "picture" trained (52- by 55-element input) binary-out and analog-out networks, respectively. Figures 10 and 11 show results for the "line" trained (5- by 52-element input) binary-out and analog-out networks, respectively. Figure 12 shows results for the picture trained (52- by 55-element) analog-out network, after training for a short time.

The networks used to generate the results for figures 8 to 11 trained perfectly, and the small solid points for the training sets lie on the measured line. The large points showing scatter and deviations are test points. The line sensor, in general, performs a little better than the picture sensor in spite of the difficulties voiced in making the line measurements. The line trained networks need to consider fewer extraneous pixels than the picture trained networks. A large number of extraneous pixels (pixels not located in the region being measured) will increase the sensitivity of the sensor to noise. Networks where all the input nodes are related to the output nodes have shown excellent noise immunity (ref. 4).

Direct tests of noise immunity and repeatability were not included in this demonstration. There is indirect evidence for lower noise immunity and immunity to extraneous systematic effects than might be desired. This evidence includes the scatter of test points located between perfectly learned training points.

Also, the networks did not learn to extrapolate very well. The picture trained net with analog output (fig. 9) has the best performance. It predicts the correct measured value of 19 pixels at 65 psig, and a value of 43 pixels at 120 psig which differs from the measured value by -3 pixels. The picture trained net with binary output (fig. 8) has errors of $+4$ and -9 pixels, respectively, even though it performs better in the calibration region. The line trained net with analog output (fig. 11) differed from the measured values

by +4 pixels at 65 psig and −8 pixels at 120 psig. The line trained net with binary output (fig. 10) had the worst extrapolation record overall with errors of +10 and −10 pixels, respectively.

The measurement and training processes show systematic and anomalous effects. The measured curves for the picture sensor and line sensor differ by 2 pixels at the low pressure end and by 4 pixels at the high pressure end. Training involves a number of adjustable parameters and requires a certain amount of trial and error. The results can vary. The result for the picture trained net with analog output (fig. 9) shows a number of test points deviating from the measured curve in an apparently systematic manner. A copy of this net was trained again for a very short time, and the result is shown in figure 12. Both the training and test points deviate from the measured curve here, but the effects seen in figure 9 are absent. The short-time trained net does not extrapolate well at all: it yields values of 26 and 22 pixels at 65 and 120 psig, respectively. The nets with binary outputs show a few outlying points. Figure 10 shows a point with a particularly large deviation. The binary digits as produced by the net show a certain amount of scatter depending on the training error as explained in the previous section. The digits are rounded up to 1 or down to 0 for the output. The scatter does not depend on the significance of the digit. The very erroneous point in figure 10 contained an error in the fifth bit resulting in a deviation of 16 pixels.

This demonstration leads to a number of conclusions and suggestions.

CONCLUDING REMARKS

Glancing at the input pictures in figure 4 followed by the result of calibration for the shock wave position in figure 8 should make the major point of this paper: artificial neural networks have the potential to automate the "semiquantitative" function of flow visualization in aeronautics.

Weighing everything, the neural networks achieved the calibration objectives stated under **CALIBRATION AND TRAINING**. The networks learned the training examples precisely; some of the networks did a good job of interpolation; and one network did a fair job of extrapolation.

Nevertheless, this paper contains by no means a complete or carefully done study. The shock waves shown in figure 4 change both shape and position as the pressure is varied. The neural network is receiving information about the entire shock wave, yet the position is measured at a single point on the shock front. A better study would have used a carefully constructed nozzle and would have measured the geometry of the entire shock front. That geometry would have been encoded either as position measurements or as parameters for a curve fit of the shock wave.

It is particularly important to test the resistance of the calibration to noise and certain systematic effects. Neural networks automatically learn relationships. The great danger is that the neural network will learn the wrong relationship. Suppose, for example, that a careless experimenter adjusts his illumination in some systematic manner between frames. The experimenter then measures the shock wave position in the manner of this demonstration and does a picture to position calibration. It is quite possible that the network will learn the correlation between the illumination pattern and the shock position. There is a real correlation, since the experimenter changed the illumination pattern and shock position together. But, that is not what he wanted the network to learn.

Training a neural network correctly is similar to teaching a technique to a person: provide consistent, correct examples. Neural networks learn what you do and not what you say, unlike expert systems. A more correct procedure might be to teach the neural network the measurement technique actually used by the operator. This technique consisted in moving a line (cropping) until that line coincided with the edge

of a shadow (shock front). This procedure involved a sequence of moves determined by human judgement. Neural networks or fuzzy control packages are easily taught to perform such sequences as demonstrated by the automation of the optical alignment process (ref. 1). However, intelligent sequencers (human or machine) are slow, so the calibration method is probably preferable.

These remarks indicate that the correct way to apply neural networks is to have the job done by an expert in the application who knows something about artificial neural networks rather than by an expert in neural networks. Experts in neural networks develop hardware, convenient-to-use software, faster training algorithms, new architectures, the philosophy of neural networks, and the like.

These remarks and results lead us to the following conclusions and recommendations. This shock wave demonstration can serve as guidance to further work on any specific optical system. The calibration procedure is best accomplished in the facility where it will be used. Collecting frames of flow visualization data is not difficult. Adapting neural network calibrations to these facilities is a matter of on-site time and effort.

Optical instrumentation specialists can make a contribution to the neural network technology. As stated in the introduction, we have projects in progress on automated alignment, processing of optical data, and wind tunnel operations. There is another important question: are there measurement processes requiring whole field optical detection that are sufficiently adaptable from one facility to another that justify the creation of a central calibration development and service effort? Such measurement processes probably would use fiber optic imaging. An example would be a probe that recognizes various kinds of cracking and takes appropriate action based on the crack type.

REFERENCES

1. Decker, A.J.; and Krasowski, M.J.: Neural Nets for Aligning Optical Components in Harsh Environments—Beam Smoothing Spatial Filter as an Example. Structural Integrity and Durability of Reusable Space Propulsion Systems, NASA CP–10064, 1991, pp. 29–38.

2. Decker, A.J.: Self-Aligning Optical Measurement Systems. Applied Optics, vol. 31, no. 22, 1992, pp. 4339–4340.

3. Decker, A.J.; Krasowski, M.J.; and Weiland, K.E.: Neural Network Directed Alignment of Optical Systems Using the Laser-Beam Spatial Filter as an Example. To be published as a NASA TP, 1993.

4. Decker, A.J.; and Krasowski, M.J.: General Procedure for Using Artificial Neural Networks to Automate the Alignment of Optical Components in Harsh Environments. Advanced Earth-to-Orbit Propulsion Technology 1992, NASA CP–3174, vol. I, 1992, pp. 303–312.

5. Krasowski, M.J.; and Dickens, D.E.: A Fuzzy Logic Based Controller for the Automated Alignment of a Laser-Beam-Smoothing Spatial Filter. NASA TM–105994, 1992.

6. Decker, A.J.: Neural Networks for Calibration Tomography. To be presented at SPIE's 1993 International Symposium on Optical Applied Science and Engineering, Conference on Optical Diagnostics in Fluid and Thermal Flow, San Diego, CA, July 11–16, 1993.

7. Troudet, T.; and Merrill, W.C.: Neuromorphic Learning of Continuous-Valued Mappings From Noise-Corrupted Data, Application to Real-Time Adaptive Control. NASA TM–4176, 1990.

8. McCulloch, W.S.; and Pitts, W.: A Logical Calculus of the Ideas Immanent in Nervous Activity. Bulletin of Mathematical Biophysics, vol. 5, 1943, pp. 115–133.

9. Zadeh, L.A.: Fuzzy Sets. Information and Control, vol. 8, 1965, pp. 338–353.

10. Iverson, D.G. Jr.; and Daiber, T.D.: Flight Prototype Normal Shock Sensor. NASA CR–185204, 1989.

11. Hesse, W.J.; and Mumford, N.V.S., Jr.: Jet Propulsion for Aerospace Applications. Pitman Publishing Corporation, 1964, pp. 136–141.

12. Merzkirch, W.: Flow Visualization. Academic Press, 1987, pp. 126–134.

13. COHU Model 4815 Solid-State Monochrome CCD Camera, vended by COHU, Inc., 5755 Kearny Villa Road, San Diego, CA 92123, and 85-250 mm Olympus zoom lens with c-mount adapter and 20 mm extension tube.

14. PIP–512B Video Digitizer Board for the IBM PC, XT, and AT, vended by MATROX Electronic Systems Limited, 1055 St Regis Blvd., Dorval, Quebec, Canada H9P 2T4.

15. Personal Iris Model 4D/25TG, vended by Silicon Graphics, Inc., 2011 N. Shoreline Boulevard, Mountain View, CA 94043.

16. Neural Works Professional II/PLUS, vended by Neural Ware, Inc., Penn Center West, Building IV, Pittsburgh, PA 15276.

17. Rumelhart, D.E.; McClelland, J.L.; and the PDP Research Group: Parallel Distributed Processing—Explorations in the Microstructure of Cognition, Volume 1: Foundations. MIT Press, 1986.

18. Pao, Y.-H.: Adaptive Pattern Recognition and Neural Networks. Addison-Wesley, 1989.

19. Padgett, M.L.: Workshop on Neural Networks: Academic/Industrial/NASA/Defense, Society for Computer Simulation International, 1991.

20. Ruck, D.W., et al.: The Multilayer Perceptron as an Approximation to a Bayes Optimal Discriminant Function. IEEE Transactions on Neural Networks, vol. 1, 1990, pp. 296–298.

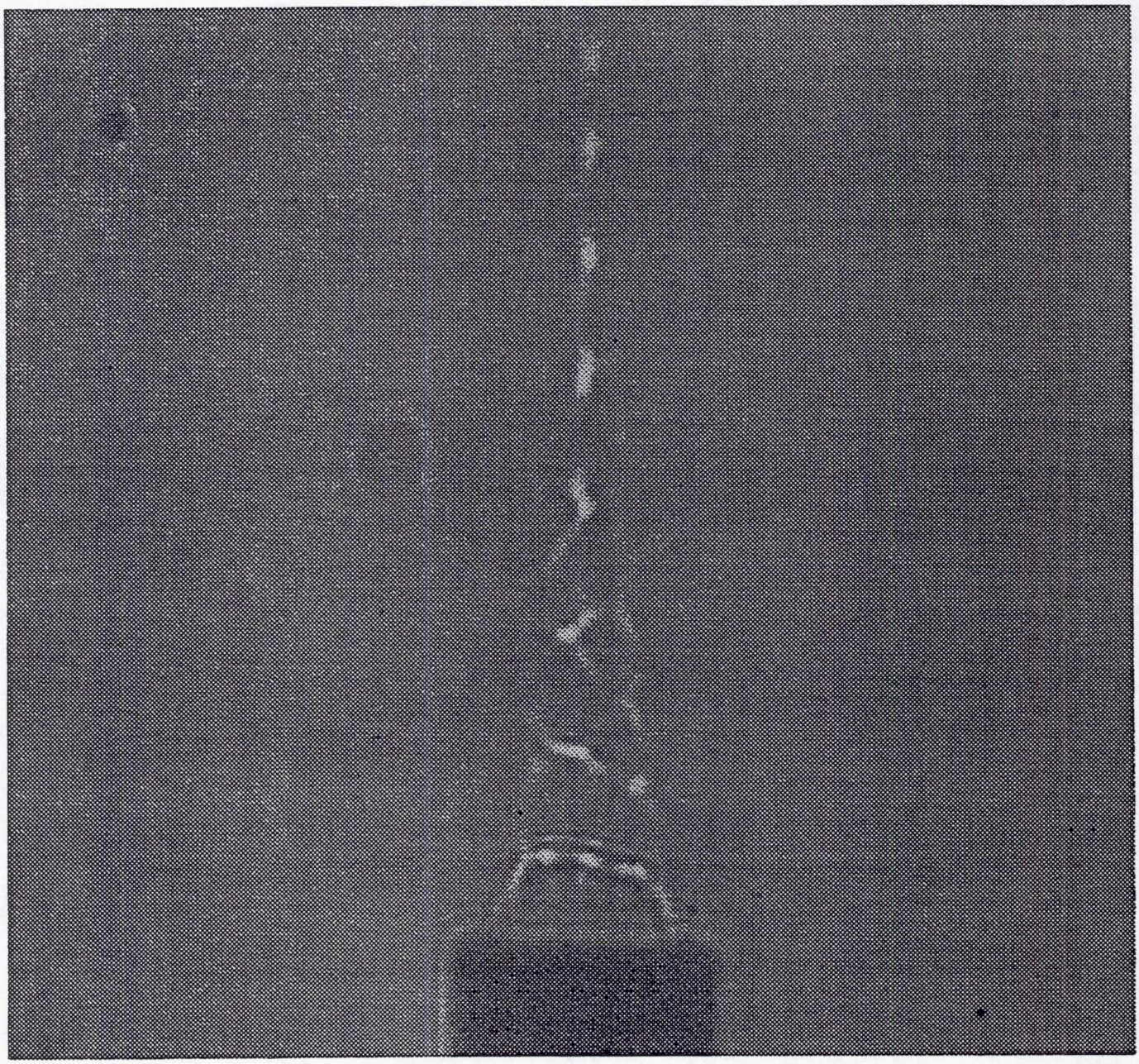

Figure 1.—Shadowgraph of shock structure from supercritically operated nozzle as recorded by CCD camera.

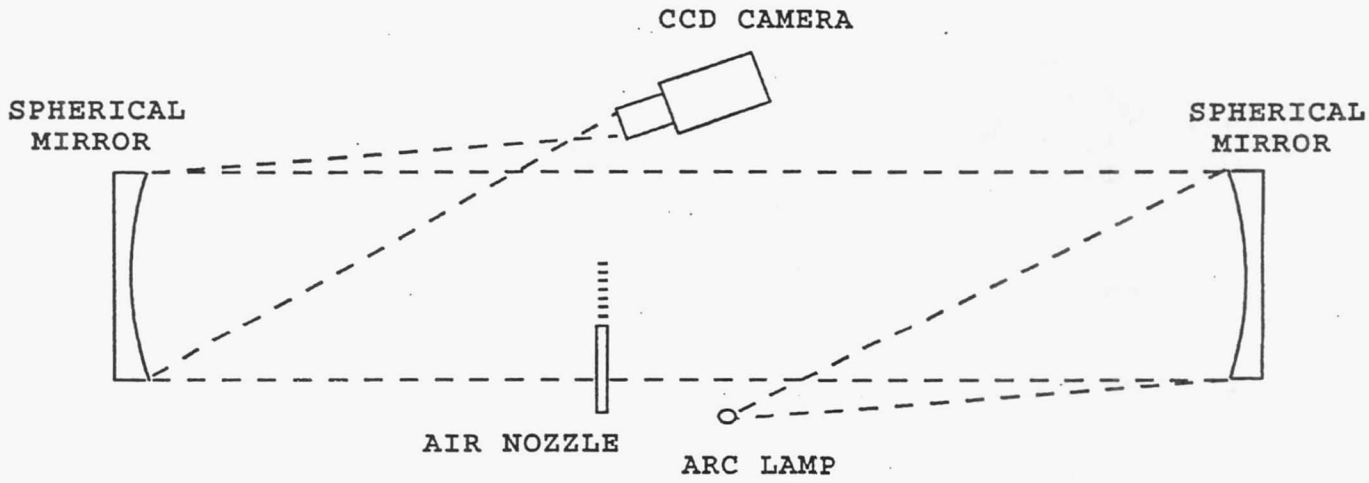

Figure 2.—Schematic of shadowgraph used to visualize shock waves and record their shadows.

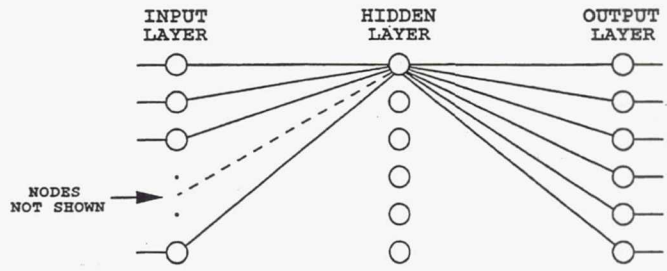

Figure 3.—Standard feedforward neural network: signals proceed from inputs at left to outputs at right, and connections are shown only to and from one node in hidden layer.

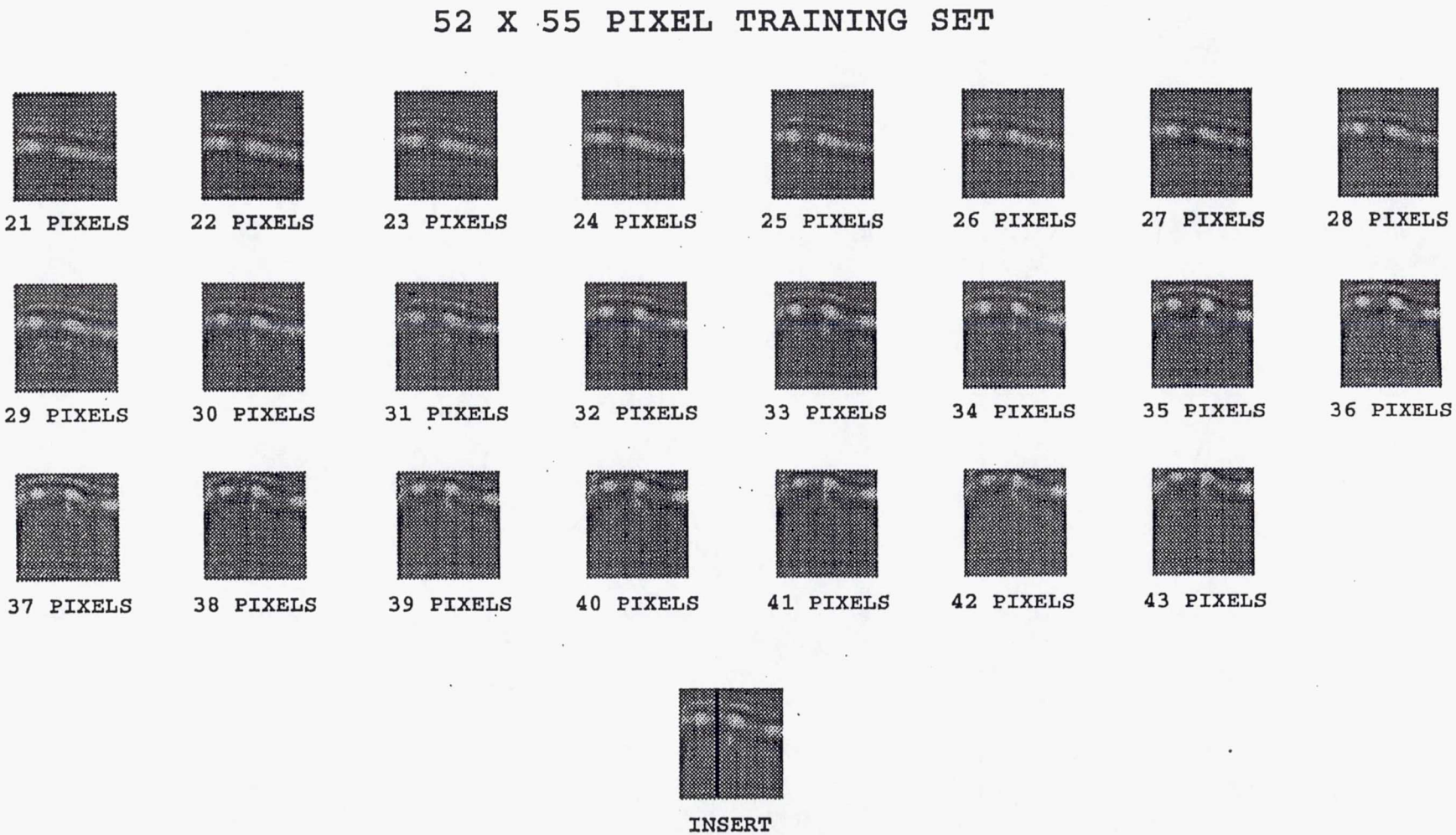

Figure 4.—Training inputs: the y-distance of the measured point above the nozzle is stated in pixels, and the region measured is centered about the line through the insert. The tube pressure varies in 2 psi increments as the y-distance varies from 21 pixels to 43 pixels.

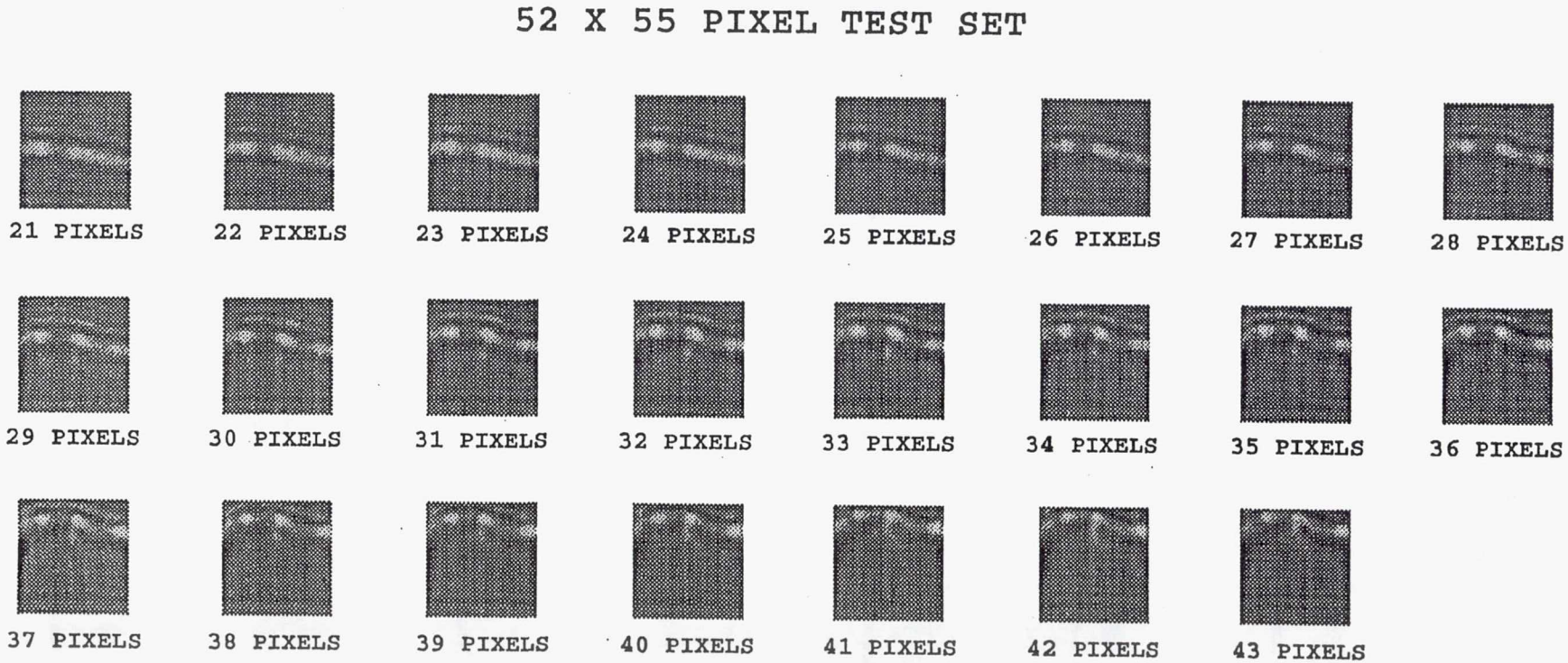

Figure 5.—Test inputs; description is identical with that of Figure 4.

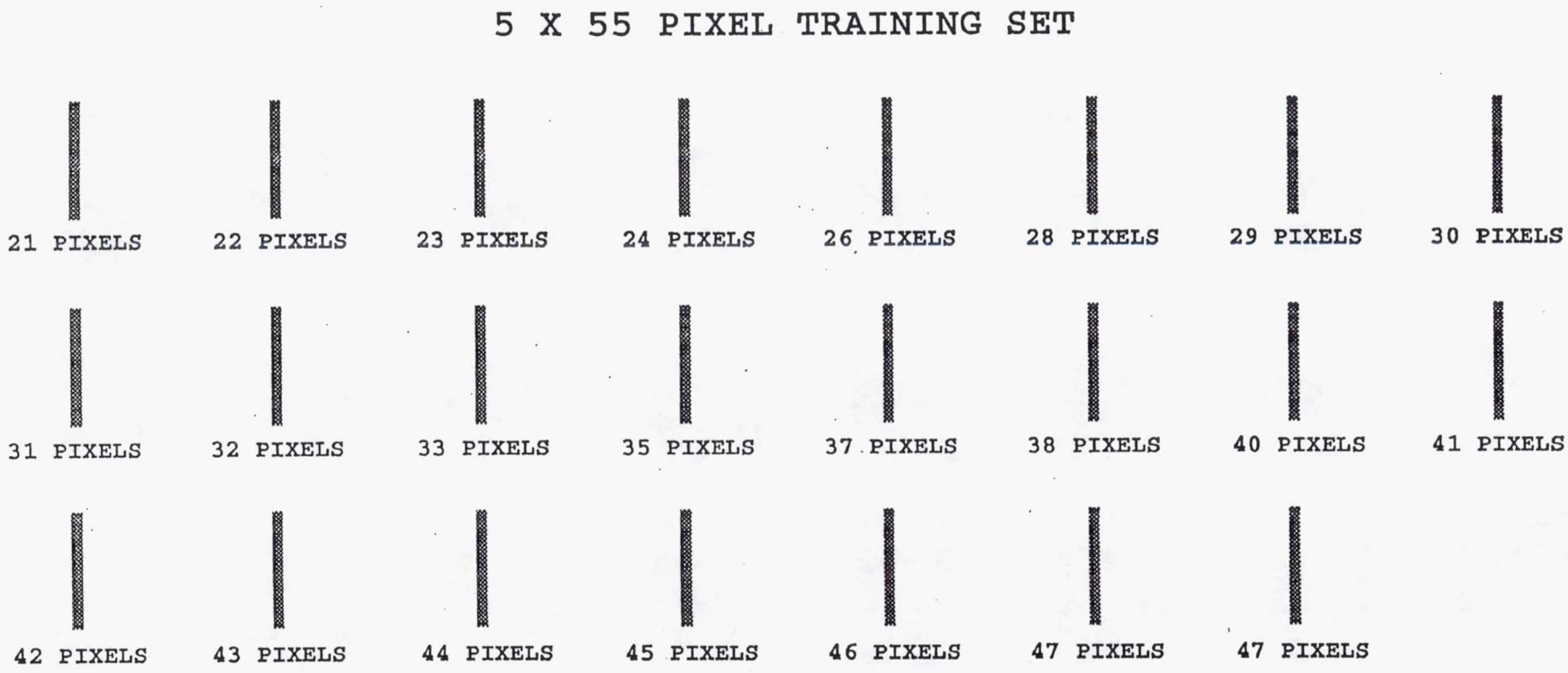

Figure 6.—Training inputs reduced to approximate line-sensor format.

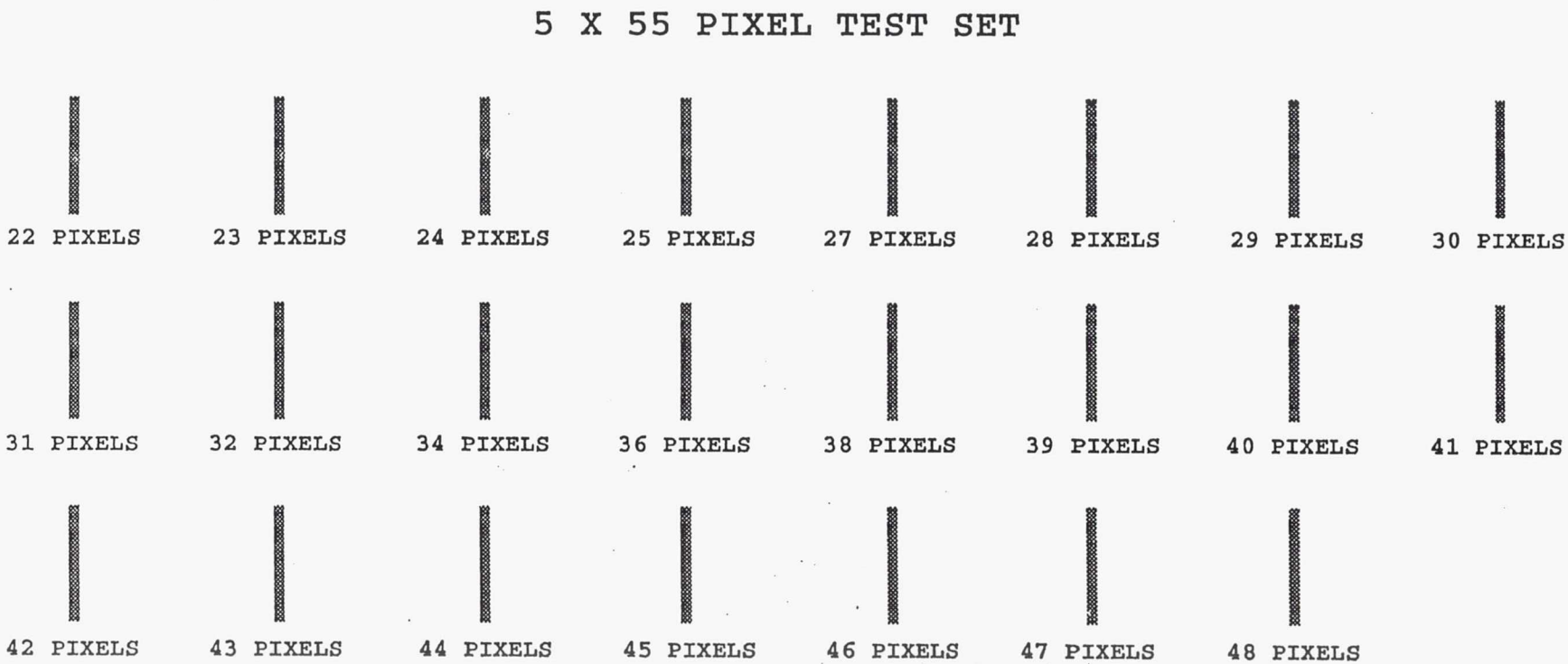

Figure 7.—Test inputs reduced to approximate line-sensor format.

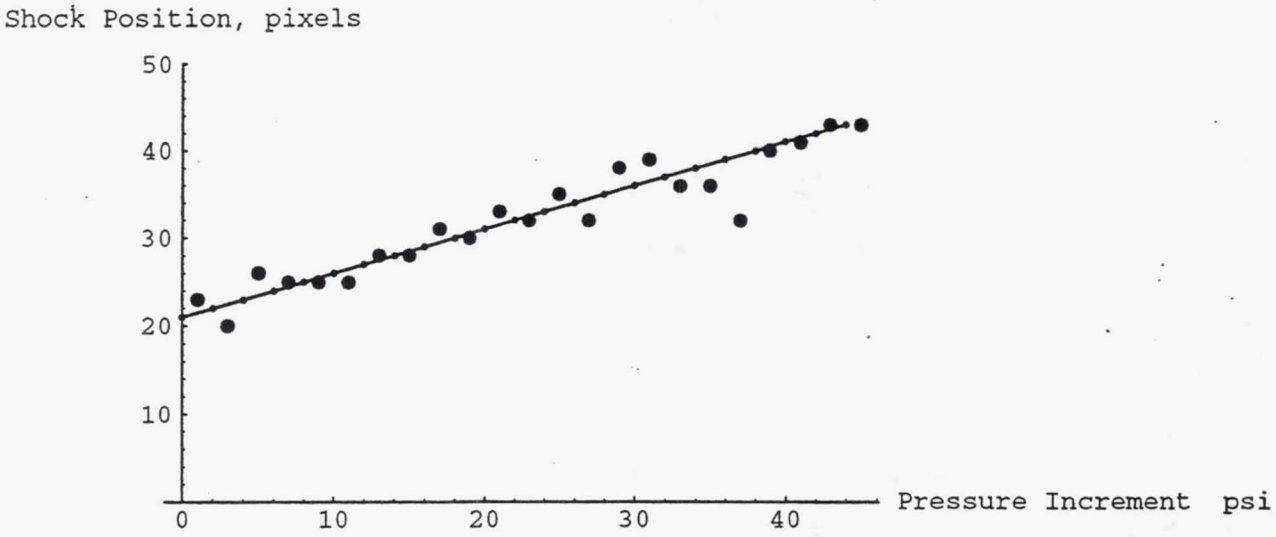

Figure 8.—Result of calibration with 52 x 55 pixel inputs and binary outputs; solid line was measured; dots were network generated where small dots represent training inputs and large dots represent test inputs.

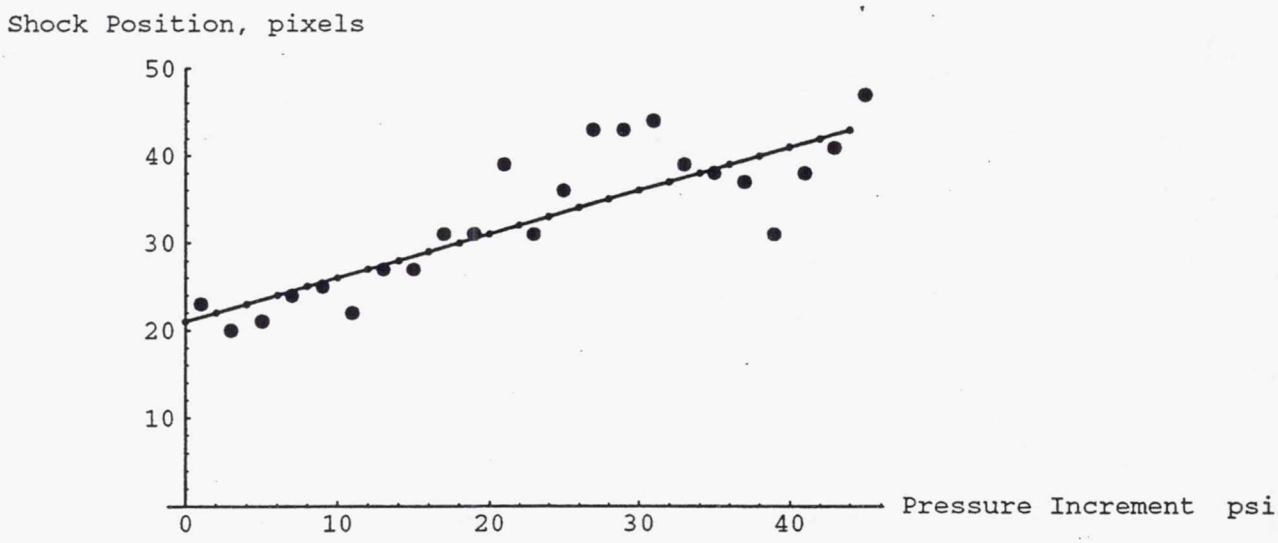

Figure 9.—Result of calibration with 52 x 55 pixel inputs and analog outputs; solid line was measured; dots were network generated where small dots represent training inputs and large dots represent test inputs.

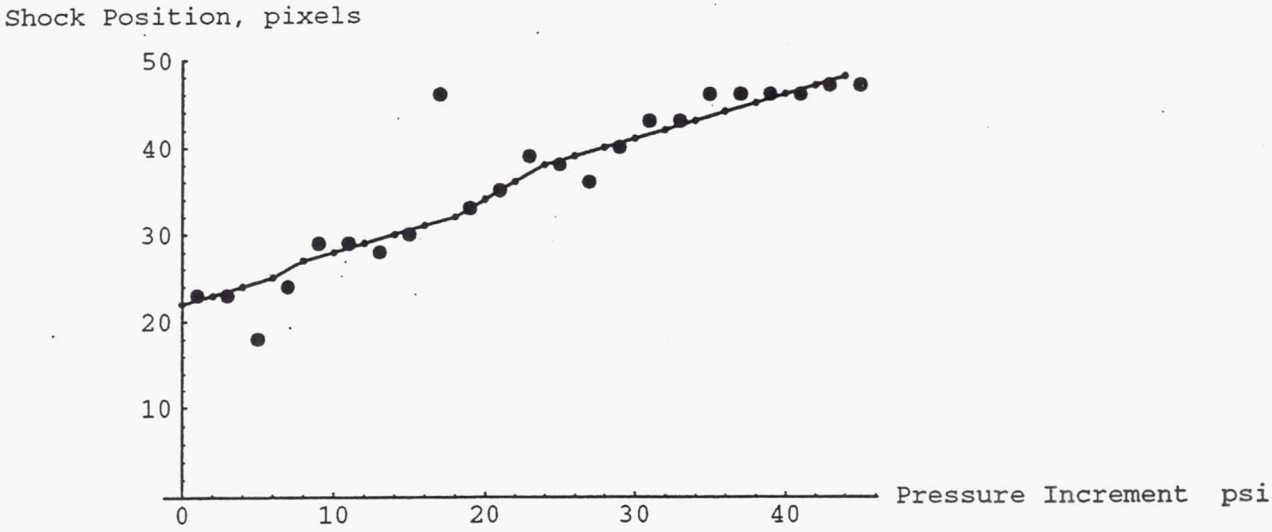

Figure 10.—Result of calibration with 5 x 55 pixel simulated line inputs and binary outputs; solid line was measured; dots were network generated where small dots represent training inputs and large dots represent test inputs.

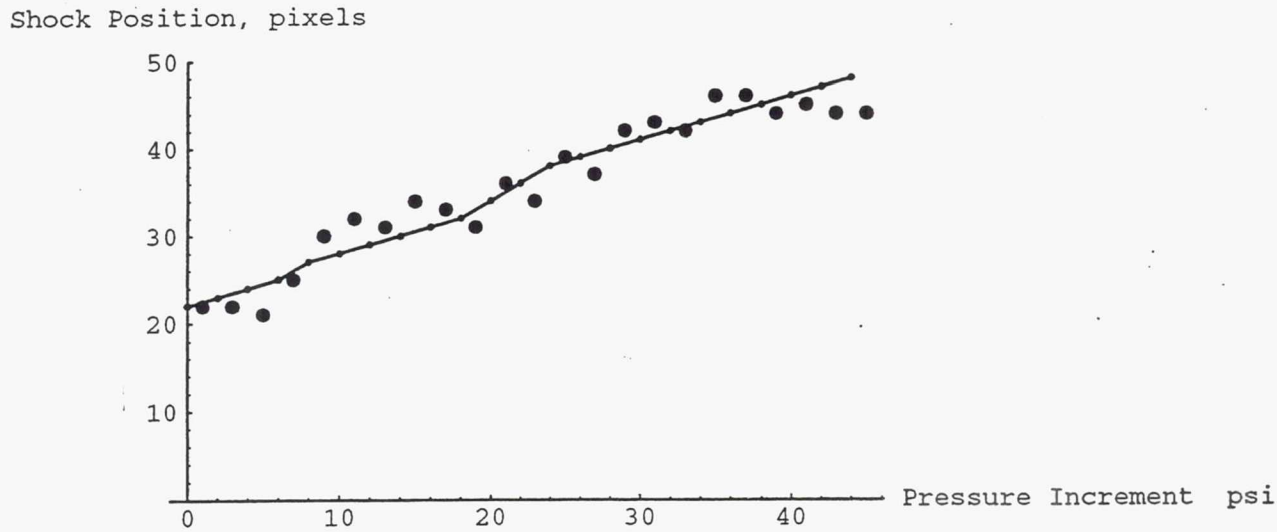

Figure 11.—Result of calibration with 5 x 55 pixel simulated line inputs and analog outputs; solid line was measured; dots were network generated where small dots represent training inputs and large dots represent test inputs.

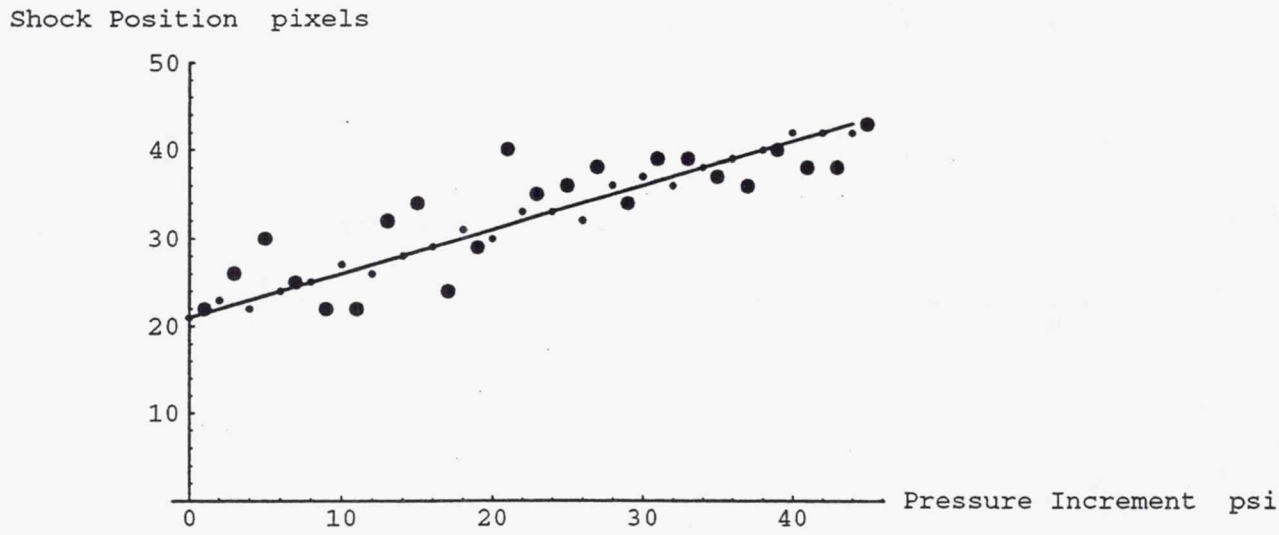

Figure 12.—Calibration as in Figure 9, but with shorter training period. Note that small dots representing training inputs do not all lie on the measured line as in previous figures.

REPORT DOCUMENTATION PAGE

Form Approved
OMB No. 0704-0188

1. AGENCY USE ONLY (*Leave blank*)	2. REPORT DATE	3. REPORT TYPE AND DATES COVERED
	May 1993	Technical Memorandum

4. TITLE AND SUBTITLE

Calibration of a Shock Wave Position Sensor Using Artificial Neural Networks

5. FUNDING NUMBERS

WU–505–62–50

6. AUTHOR(S)

Arthur J. Decker and Kenneth E. Weiland

7. PERFORMING ORGANIZATION NAME(S) AND ADDRESS(ES)

National Aeronautics and Space Administration
Lewis Research Center
Cleveland, Ohio 44135–3191

8. PERFORMING ORGANIZATION REPORT NUMBER

E–7819

9. SPONSORING/MONITORING AGENCY NAME(S) AND ADDRESS(ES)

National Aeronautics and Space Administration
Washington, D.C. 20546–0001

10. SPONSORING/MONITORING AGENCY REPORT NUMBER

NASA TM–106138

11. SUPPLEMENTARY NOTES

Responsible person, Arthur J. Decker, (216) 433–3639.

12a. DISTRIBUTION/AVAILABILITY STATEMENT

Unclassified - Unlimited
Subject Category 35

12b. DISTRIBUTION CODE

13. ABSTRACT ***(Maximum 200 words)***

This report discusses the calibration of a shock wave position sensor. The position sensor works by using artificial neural networks to map cropped CCD frames of the shadows of the shock wave into the value of the shock wave position. This project was done as a tutorial demonstration of method and feasibility. It used a laboratory shadowgraph, nozzle, and commercial neural network package. The results were quite good, indicating that artificial neural networks can be used efficiently to automate the semiquantitative applications of flow visualization.

14. SUBJECT TERMS

Shock wave position measurements; Artificial neural networks; Shadowgraph; Flow visualization

15. NUMBER OF PAGES

20

16. PRICE CODE

A03

17. SECURITY CLASSIFICATION OF REPORT	18. SECURITY CLASSIFICATION OF THIS PAGE	19. SECURITY CLASSIFICATION OF ABSTRACT	20. LIMITATION OF ABSTRACT
Unclassified	Unclassified	Unclassified	

National Aeronautics and
Space Administration

Lewis Research Center
Cleveland, Ohio 44135